Discrete solitons in $\mathcal{PT}$-symmetric lattices

V. V. Konotop[1], D. E. Pelinovsky[2] and D. A. Zezyulin[1]

[1] *Centro de Física Teórica e Computacional and Departamento de Física, Faculdade de Ciências,*
Universidade de Lisboa - Avenida Professor Gama Pinto 2, Lisboa 1649-003, Portugal, EU
[2] *Department of Mathematics and Statistics, McMaster University - Hamilton, Ontario, L8S 4K1, Canada*

Abstract – We prove the existence of discrete solitons in infinite parity-time ($\mathcal{PT}$) symmetric lattices by means of analytical continuation from the anticontinuum limit. The energy balance between dissipation and gain implies that in the anticontinuum limit the solitons are constructed from elementary $\mathcal{PT}$-symmetric blocks such as dimers, quadrimers, or more general oligomers. We consider in detail a chain of coupled dimers, analyze bifurcations of discrete solitons from the anticontinuum limit and show that the solitons are stable in a sufficiently large region of the lattice parameters. The generalization of the approach is illustrated on two examples of networks of quadrimers, for which stable discrete solitons are also found.

Introduction. – Energy localization in lattices is a fundamental topic. It received particular attention after the prediction of the intrinsic localized modes [1] and the subsequent rigorous proof of the existence of such modes [2] by analytical continuation from the anticontinuum limit when the coupling of the nearest neighbors is weak. Nowadays the topic is very well elaborated and numerous physical applications, including nonlinear optics [3] and Bose-Einstein condensates [4], have been thoroughly studied. One of the most popular models appearing in the description of these physical phenomena, which is also a widely accepted testbed for mathematical analysis of the anticoninuum limit, is the discrete nonlinear Schrödinger (DNLS) equation [5], also known as the discrete self-trapping equation [6].

More recently, particular attention was paid to the DNLS equation with gain and losses. Such models naturally appear in the optical context of arrays of amplifying and absorbing waveguides [7]. If gain and losses are adjusted to create the refractive-index profile having symmetric real and anti-symmetric imaginary parts [8], such systems have parity-time ($\mathcal{PT}$) symmetry and may have a pure real spectrum. Originally the idea about the existence of a pure real spectrum of complex potentials obeying the $\mathcal{PT}$ symmetry was introduced in [9] questioning the fundamentals of the quantum mechanics. It turned out, however, that the most direct applications of the $\mathcal{PT}$ symmetry today can be found in the discrete optics. Namely, in such systems, and more specifically

in two coupled waveguides (one with dissipation and another with gain), the phenomenon was implemented experimentally [10].

Many detailed studies of $\mathcal{PT}$-symmetric DNLS equation were already developed for lattices with a finite number of sites. In particular, the following topics have been considered: periodic oscillations in a system of two oscillators (a *dimer*) [11]; stationary nonlinear modes for four oscillators (a *quadrimer*) [12,13]; the relation between one- and two-dimensional finite $\mathcal{PT}$-symmetric networks [13], and the detailed analysis of two-dimensional plaquettes [14]. The transition to the limit of an infinite number of sites was investigated in [15]. It was shown that in this limit the $\mathcal{PT}$ symmetry breaking occurs at gain-loss coefficient approaching zero. Stable discrete solitons in the infinite chain of $\mathcal{PT}$-symmetric DNLS oscillators with alternating coupling were discovered numerically in [16]. However, the solitons obtained in [16], displayed oscillations and neither analytical proof of the existence nor the number of possible families of solutions were clarified, so far.

In this letter, we give an analytical proof of the existence of discrete solitons in $\mathcal{PT}$-symmetric DNLS lattices with alternating coupling coefficients and classify different solution families and their stability near the anticontinuum limit. In particular, we report multistability of localized modes, that is, the existence of two or more stable solutions with the same energy and the same lattice parameters (but having different shapes).
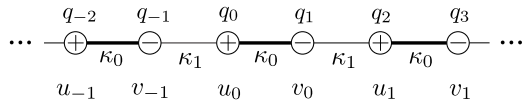
Fig. 1: Schematic presentation of the $\mathcal{PT}$-symmetric array of waveguides with gain ("+"), and losses ("−"), and with the notations used in the text.

The DNLS equation with alternating coefficients of gain and loss can be viewed is a discrete (tight-binding) limit of a continuous $\mathcal{PT}$-symmetric lattice. Stable solitons in such systems have been found in the presence of only linear [17], only nonlinear [18], and both linear and nonlinear [19] $\mathcal{PT}$ lattices. The solutions considered in this letter can be viewed as discrete counterparts of the mentioned solitons.

We consider the $\mathcal{PT}$-symmetric DNLS equation

$$i\frac{\mathrm{d}q_n}{\mathrm{d}t} + c_n(q_{n+1} - q_n) + c_{n+1}(q_{n-1} - q_n) - g|q_n|^2 q_n$$
$$+ i(-1)^{n+1}\gamma q_n = 0, \tag{1}$$

where the positive constants $c_n = \kappa_0$ for $n = 2p$ and $c_n = \kappa_1$ for $n = 2p+1$ describe the two alternating couplings (κ_0 and κ_1, with $\kappa_{0,1} > 0$) between neighbor sites, and it is assumed that all odd (even) sites have loss (gain) which is characterized by the factor $\gamma > 0$ (see fig. 1). In the context of optical applications our model describes an array of waveguides with gain and losses. Then q_n is a dimensionless field in the waveguide n, and t stands for the propagation coordinate.

Let us first briefly address the most important features of the underlying linear problem, which can be formally obtained from eq. (1) by setting $g = 0$. Identifying the solutions of the linear problem in the form of Floquet-Bloch modes $(q_{2n}, q_{2n+1}) = (u, v)e^{ikn - i(\kappa_0 + \kappa_1 + \mu)t}$, one can recover that $\mathcal{PT}$ symmetry is unbroken on the infinite lattice if [16]

$$|\kappa_0 - \kappa_1| \geqslant \gamma. \tag{2}$$

In this case for any real k the corresponding eigenvalue μ is real. More precisely μ^2 lies in the interval

$$(\kappa_0 - \kappa_1)^2 - \gamma^2 < \mu^2 < (\kappa_0 + \kappa_1)^2 - \gamma^2, \tag{3}$$

i.e., μ belongs either to a positive or to a negative spectrum band. If inequality (2) does not hold, we say that $\mathcal{PT}$ symmetry is broken as there exist eigenvalues μ with nonzero imaginary parts.

Returning to the nonlinear problem, without loss of generality we impose $g = \pm 1$. Furthermore, by analogy with the conservative DNLS equation (see, *e.g.*, [20]), one can verify that there exists the symmetry reduction as follows. If q_n is a solution of (1) for $g = 1$, then $(-1)^n \bar{q}_n e^{-2i(\kappa_0 + \kappa_1)t}$ is a solution of (1) for $g = -1$. This reduction allows us to restrict further considerations to the case of $g = 1$ only.

Anticontinuum limit. − We are concerned with the stationary solutions, *i.e.*, solutions whose dependence on

time is given by $q_n(t) \sim e^{-iEt}$, where E is a constant which is termed an energy (or a propagation constant in optical applications). Then, in the case of the conservative DNLS equation, the anticontinuum limit corresponds either to a coupling between the two neighbor sites tending to zero or to the energy tending to the infinity, the two limits being equivalent, *i.e.*, mapped to each other by simple transformation (see, *e.g.*, [20]). The same is true for the model (1), however with two important changes.

First, in the presence of the dissipative term $i(-1)^n\gamma q_n$ the elementary cell of the DNLS equation (1) is composed of two sites, one with gain and the other one with loss (even if $\kappa_0 = \kappa_1$). Therefore, the anticontinuum limit must be formulated in terms of dimers, rather than single sites. Thus, the anticontinuum limits can be identified as either κ_0 or κ_1 to be small enough. Without loss of generality, we fix $\kappa_0 = 1$. Then the anticontinuum limit corresponds to $\kappa_1 = 0$.

In physical applications, both coupling constants κ_0 and κ_1 are usually fixed. Then the anticontinuum limit can be realized at the limit of large energy E. However, and this is the second distinction from the conservative DNLS equation, although the small parameter can be obtained in the limit of large energy, E cannot be scaled out from the main equations if $\gamma \neq 0$.

Using the above considerations, it is convenient to rewrite the main model (1) in terms of variables

$$\begin{pmatrix} q_{2n}(t) \\ q_{2n+1}(t) \end{pmatrix} = \begin{pmatrix} u_n \\ v_n \end{pmatrix} e^{-i(\kappa_0 + \kappa_1 + \mu)t}, \tag{4}$$

where μ is a constant and we assume that u_n and v_n do not depend on t and satisfy zero boundary conditions: $u_n, v_n \to 0$ as $n \to \pm\infty$. Then for $\kappa_0 = 1$, $\kappa_1 = \epsilon$, and $g = 1$, the main model can be rewritten in the matrix form for $\boldsymbol{w}_n = (u_n, v_n)^T$ ("*T*" stands for the matrix transposition):

$$H\boldsymbol{w}_n + \epsilon\left(\sigma_- \boldsymbol{w}_{n-1} + \sigma_+ \boldsymbol{w}_{n+1}\right) = F(\boldsymbol{w}_n)\boldsymbol{w}_n, \tag{5}$$

where

$$H = \begin{pmatrix} \mu - i\gamma & 1 \\ 1 & \mu + i\gamma \end{pmatrix},$$

$$\sigma_- = \begin{pmatrix} 0 & 1 \\ 0 & 0 \end{pmatrix}, \quad \sigma_+ = \begin{pmatrix} 0 & 0 \\ 1 & 0 \end{pmatrix},$$

and $F(\boldsymbol{w}_n) = \mathrm{diag}(|u_n|^2, |v_n|^2)$.

Single-dimer state. − First, we address the simplest case in which only one central dimer is excited in the anticontinuum limit $\epsilon = 0$, *i.e.*, $\boldsymbol{w}_0 \neq 0$, whereas $\boldsymbol{w}_n = 0$ for $n \neq 0$. Then for any $n \neq 0$ eq. (5) is automatically satisfied. For the central dimer, *i.e.*, at $n = 0$, we assume that the following $\mathcal{PT}$ symmetry reduction holds: $u_0 = \bar{v}_0$ and arrive at the following equation [11]:

$$(\mu - i\gamma)u_0 + \bar{u}_0 = |u_0|^2 u_0. \tag{6}$$

The latter equation has two branches of solutions, which exist for all $\gamma \in [0, 1)$:

$$u_0^\pm = A_\pm e^{i\varphi_\pm}, \tag{7}$$

where $A_\pm^2 = \mu \pm \sqrt{1-\gamma^2}$, $\sin(2\varphi_\pm) = -\gamma$, and $\cos(2\varphi_\pm) = \pm\sqrt{1-\gamma^2}$. The branches $u_0^\pm$ exist for $\mu > \mu_\pm$ where $\mu_\pm = \pm\sqrt{1-\gamma^2}$. The physical difference between these branches becomes evident if we introduce the linear momentum $p_n = 2\mathrm{Re}\,(\bar{q}_n q_{n+1})$ and the current $j_n = 2\mathrm{Im}\,(\bar{q}_n q_{n+1})$ per unit cell; respectively, $p = \sum_n p_n$ and $j = \sum_n j_n$ are the total momentum and current carried out by the solution. Then, branch u_0^+ (branch u_0^-) corresponds to the linear momentum and current, between the two sites of the dimer, having the same (opposite) directions. Note that eq. (6) coincides with the equation for the stationary solutions of the parametrically driven NLS equation [21,22].

Looking for continuation of the solution (7) from the anticontinuum limit (*i.e.*, from $\epsilon = 0$ to $\epsilon > 0$) it is natural to suppose that for $\epsilon > 0$ the solitons also obey the symmetry reduction on the whole infinite lattice, *i.e.*,

$$u_n = \bar{v}_{-n}, \quad v_n = \bar{u}_{-n}, \quad n = 0, \pm 1, \pm 2, \ldots . \quad (8)$$

It allows one to restrict the consideration only to $n \geqslant 0$. At the central dimer, $\boldsymbol{w}_0$, one can introduce the real coordinates (a_0, b_0) such that $u_0 = \bar{v}_0 = a_0 + ib_0$ and rewrite (5) for $n = 0$ as follows:

$$\begin{cases} \mu a_0 + \gamma b_0 + a_0 + \epsilon \mathrm{Re}(u_1) = (a_0^2 + b_0^2)a_0, \\ \mu b_0 - \gamma a_0 - b_0 - \epsilon \mathrm{Im}(u_1) = (a_0^2 + b_0^2)b_0. \end{cases} \quad (9)$$

For $n \geqslant 1$, we still use the complex-valued coordinates:

$$\begin{cases} (\mu - i\gamma)u_n + v_n + \epsilon v_{n-1} = |u_n|^2 u_n, \\ (\mu + i\gamma)v_n + u_n + \epsilon u_{n+1} = |v_n|^2 v_n. \end{cases} \quad (10)$$

Now the system (9), (10) is smooth with respect to parameter ϵ and the solution vector. At $\epsilon = 0$, we have the limiting solution: $u_n = v_n = 0$ for all $n = 1, 2, \ldots$, while a_0 and b_0 are given by one of the two possible solutions (7) for $\gamma \in [0, 1)$ and $\mu > \mu_\pm$. To apply the implicit function theorem arguments, we need to show that the Jacobian operator of the system (9), (10) at $\epsilon = 0$ is invertible at the limiting solution. Furthermore, the solution can be analytically continued from the anticontinuum limit until a critical value $\epsilon_{cr} > 0$ for which the Jacobian operator becomes non-invertible.

In the case of the conservative DNLS equation ($\gamma = 0$) analytical estimates for ϵ_{cr} can be obtained [2,20]. While such estimates require elaborated analytical study, due to mathematical constraints they are typically lower than the practically achievable values of ϵ for which the localized solutions exist. Therefore, here we restrict the consideration only to the proof that the analytical continuation is possible and study the continuation numerically.

For $\epsilon = 0$, the lattice consists of a set of uncoupled dimers. For $n = 1, 2, \ldots$, the limiting Jacobian operator of the system (10) is nothing but H and thus is invertible for $\mu \neq \mu_\pm$ since $\det(H) = \mu^2 + \gamma^2 - 1$.

At the central dimer $n = 0$, the limiting Jacobian operator of the system (9) is given by the 2×2 matrix:

$$J_0 = \begin{pmatrix} -2a_0^2 - \gamma b_0/a_0 & \gamma - 2a_0 b_0 \\ -\gamma - 2a_0 b_0 & -2b_0^2 + \gamma a_0/b_0 \end{pmatrix}, \quad (11)$$

where eq. (6) has been used. The matrix J_0 is invertible if $a_0 b_0 \neq 0$ and $a_0^2 \neq b_0^2$. This gives the constraints $A_\pm \neq 0$ and $\cos(2\varphi_\pm) \neq 0$ in the limiting solution (7), or equivalently, $A_\pm^2 \neq \{0, \mu\}$. The constraints are satisfied for any $\gamma \in [0, 1)$ and $\mu \neq \mu_\pm$. Hence, for any γ and μ that satisfy the found invertibility conditions, solutions $u_0^\pm$ of the dimer problem give birth to two branches of localized discrete solitons on the infinite $\mathcal{PT}$-symmetric lattice. These branches, which will be respectively denoted as $\Gamma^{(\pm)}$ (see fig. 2), are parameterized by ϵ, they persist at least for all small ϵ, and for small ϵ the solitons from the branches $\Gamma^{(\pm)}$ are nearly localized at the central dimer $\boldsymbol{w}_0$.

Multi-dimer states. – One can also consider the case in which the solution in the anticontinuum limit consists of several excited dimers. Say, for the case of two dimers, one can consider branches $\Gamma^{(+,+)}$ or $\Gamma^{(-,-)}$, which at $\epsilon = 0$ correspond to two dimers occupying two consecutive central cells $n = 0$ and $n = 1$. More complex configurations consisting of N excited dimers can also be continued from the anticontinuum limit. Even more generally, there exist branches like $\Gamma^{(+,0,+)}$, $\Gamma^{(-,0,-)}$, which in the anticontinuum limit correspond to two dimers placed at $n = -1$ and $n = 1$ separated with an "empty" dimer at $n = 0$ (*i.e.*, $\boldsymbol{w}_0 = 0$ for $\epsilon = 0$). However, the continuation is not possible for arbitrary choice of N central dimers. If we consider the sequence $\boldsymbol{\alpha} = (\alpha_1, \alpha_2, \ldots, \alpha_N)$ consisting of N symbols $\alpha_{1,\ldots,N} \in \{+, -, 0\}$, then existence of the branch $\Gamma^{\boldsymbol{\alpha}}$ is only possible provided that $\alpha_p = \alpha_{N+1-p}$ for $p = 1, \ldots N$. The latter requirement ensures that the configuration, which is chosen to be continued from $\epsilon = 0$ to $\epsilon > 0$, obeys a $\mathcal{PT}$ symmetry reduction (8). For example, for $N = 3$, the family $\Gamma^{(-,+,+)}$ can not be continued from the anticontinuum limit. However the family $\Gamma^{(-,+,-)}$ does persist for small ϵ. Invertibility of the Jacobian operators corresponding to such multi-dimer solutions can be proven using similar technique as for the case $N = 1$ considered above. We note that the relevance of the symmetry properties for possibilities of continuation of the branches of soliton solutions is similar to the case of parametrically driven NLS systems [22].

Stability in the anticontinuum limit. – We shall also address linear stability of solitons belonging to the branches $\Gamma^{(\pm)}$ bifurcating from the one-dimer states in the anticontinuum limit. For $\epsilon = 0$ and $n \neq 0$, the dimers are decoupled and the stability of the zero solution is determined by the spectrum of the matrix H which has real eigenvalues if $\gamma < 1$. Hence the zero solution for $n \neq 0$ is stable. Passing from $\epsilon = 0$ to $\epsilon > 0$, eigenvalues λ group together into bands of continuous spectrum. For small positive ϵ, these bands are situated in the neutrally stable

imaginary axis, and they are separated from each other and from zero if $\gamma \in [0, 1)$, $\mu \neq \mu_\pm$, and $\mu \neq 0$.

Thus, to ensure stability of the single-dimer soliton, we have to address only the stability of the central dimer $\boldsymbol{w}_0$. Considering a perturbed solution $\boldsymbol{w}_0 + \boldsymbol{\psi}_0 e^{\lambda t} + \overline{\boldsymbol{\psi}}_1 e^{\bar{\lambda} t}$ and linearizing the equation with respect to $\boldsymbol{\psi}_{0,1}$, for $\epsilon = 0$ we obtain the eigenvalue problem

$$\begin{pmatrix} L_0 & L_1 \\ -\bar{L}_1 & -\bar{L}_0 \end{pmatrix} \begin{pmatrix} \boldsymbol{\psi}_0 \\ \boldsymbol{\psi}_1 \end{pmatrix} = i\lambda \begin{pmatrix} \boldsymbol{\psi}_0 \\ \boldsymbol{\psi}_1 \end{pmatrix}, \quad (12)$$

where $L_0 = 2 \operatorname{diag}(|u_0^\pm|^2, |u_0^\pm|^2) - H$ and $L_1 = \operatorname{diag}((u_0^\pm)^2, (\bar{u}_0^\pm)^2)$, where $u_0^\pm$ are defined by eq. (7) for branches $\Gamma^{(\pm)}$. Because the nonlinear system (5) admits gauge invariance, $\lambda = 0$ is a double eigenvalue of the eigenvalue problem (12). As a result, the characteristic polynomial $D(\lambda)$ can be factorized by λ^2 and reads as (see also [12]): $D(\lambda) = \lambda^2 \left(\lambda^2 + 8\sqrt{1-\gamma^2}(\sqrt{1-\gamma^2} \pm \mu/2) \right)$, where eq. (7) has been used. This expression shows that for $\epsilon = 0$ and $\epsilon \ll 1$ the solitons from branch $\Gamma^{(+)}$ are stable for any $\mu > \mu_-$ and $\gamma \in [0, 1)$. Solitons of the branch $\Gamma^{(-)}$ are stable for $\epsilon = 0$ and $\epsilon \ll 1$ only if $\mu_+ < \mu < 2\mu_+$ and unstable with a positive eigenvalue for $\mu > 2\mu_+$.

Numerical results. – Turning now to the numerical study of the discrete solitons in the infinite lattice, we have computed bifurcations of families $\Gamma^{(\pm)}$ from the anticontinuum limit $\epsilon = 0$, considered their continuations to the domain $\epsilon > 0$, and examined stability of the found solitons. The results are conveniently visualized in the plane (P, ϵ), where $P = \sum_n (|u_n|^2 + |v_n|^2)$, which in optics corresponds to the total energy flow. In fig. 2 we show the results for different μ and γ. We recall that the branch $\Gamma^{(+)}$ ($\Gamma^{(-)}$) is found by means of continuation starting from the dimer solution u_0^+ (u_0^-) given by eq. (7). We tested several values of μ and γ and in all cases numerical results for stability of the families $\Gamma^\pm$ for small ϵ were in agreement with the above linear stability analysis. For example, branch $\Gamma^{(-)}$ is stable for $\mu = 1$ and $\gamma = 0.1$, but is unstable for any other considered values of μ and γ in fig. 2.

At a certain value of $\epsilon = \epsilon_0$, the norm of the solitons belonging to the branch $\Gamma^{(-)}$ vanishes, *i.e.*, $P \to 0$. Since this is the linear limit, at the point $P = 0$ the parameters obey the relation $\mu^2 = (1 + \epsilon_0)^2 - \gamma^2$, which means that the solution branch ends up at (or bifurcates from) the edge of the linear spectrum (see eq. (3)). Respectively, $\epsilon_0 = \sqrt{\mu^2 + \gamma^2} - 1$.

Bifurcation of the discrete solitons from the edge of the linear spectrum becomes particularly evident if we employ representation on the plane (P, μ), which is to be obtained for fixed γ and ϵ. Then, as shown in fig. 3, the found discrete solitons constitute continuous families, which is a frequent feature of nonlinear $\mathcal{PT}$-symmetric systems [13]. We notice that in the context of a parametrically driven NLS system, the connection of the soliton branch with the continuous spectrum was reported in [21].
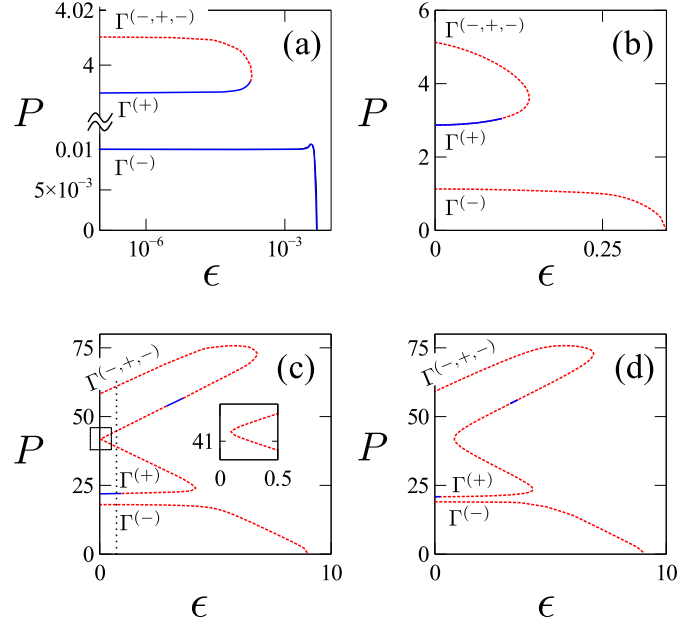

Fig. 2: (Colour on-line) P *vs.* ϵ. Panels in the top (bottom) rows correspond to $\mu = 1$ ($\mu = 10$). Panels in the left (right) column correspond to $\gamma = 0.1$ ($\gamma = 0.9$). Stable (unstable) solitons are shown by solid blue (dotted red) lines. Notice that panel (a) has a logarithmic scale in the horizontal axis and broken vertical axis. The vertical dotted line in panel (c) corresponds to $\epsilon = 0.8$; see also fig. 3.
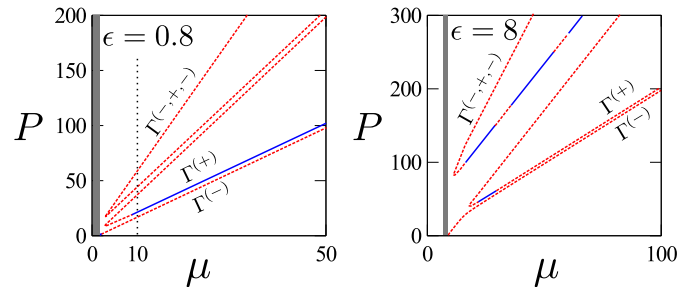

Fig. 3: (Colour on-line) P *vs.* μ for $\gamma = 0.1$ and different ϵ. Vertical shadowed domains show the bands of the linear spectrum. The vertical dotted line in the left panel corresponds to $\mu = 10$; see also fig. 2.

The branch $\Gamma^{(+)}$ is stable for sufficiently small ϵ for all considered μ and γ (in agreement with the linear stability analysis). For $\mu = 10$ (see fig. 2(c), (d)) solitons of the family $\Gamma^{(+)}$ lose stability (the part of the continuous spectrum leaves the imaginary axis and becomes unstable) at $\epsilon = 1 - \gamma$, *i.e.*, at the $\mathcal{PT}$ symmetry breaking bifurcation (see eq. (2)). At $\epsilon = 1 + \gamma$, the $\mathcal{PT}$ symmetry is restored (see eq. (2)), but the branch $\Gamma^{(+)}$ does not become stable, because isolated unstable eigenvalues persist in the spectrum of linearization. Altogether, the branch $\Gamma^{(+)}$ displays "snaking" behavior and has several alternating domains of stability and instability. Finally, branch $\Gamma^{(+)}$ returns to the anticontinuum limit by means of coalescing with the branch $\Gamma^{(-,+,-)}$ bifurcating from the three-dimer state in the anticontinuum limit.
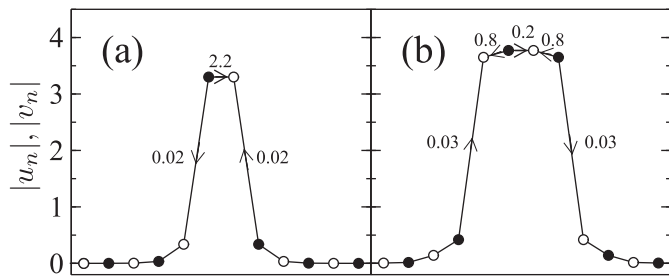
Fig. 4: Amplitude and currents for the unstable soliton at $\epsilon = 1$, $P \approx 22$ (panel (a)) and for stable soliton at $\epsilon = 3.32$, $P \approx 56$ (panel (b)). For both shown solitons $\mu = 10$ and $\gamma = 0.1$. Filled and empty circles correspond to sites with gain (i.e., u_n) and losses (i.e., v_n), respectively. Arrows show directions and amplitudes of the largest currents in the system.

For large μ, e.g., $\mu = 10$ in fig. 2(c), (d), branches $\Gamma^{(\pm)}$ can be continued into the region $\epsilon \in (1-\gamma, 1+\gamma)$, where $\mathcal{PT}$ symmetry is broken. In particular, solitons exist at $\epsilon = 1$, i.e., $\kappa_0 = \kappa_1$, (fig. 4(a)); such solitons, however, are unstable. A stable soliton is shown in fig. 4(b).

Generalizations. – The developed approach can be applied to the case when the elementary cell of a network is a more complex $\mathcal{PT}$-symmetric cluster (than the dimer). To illustrate this, we now briefly address the anticontinuum limit for two networks of quadrimers, i.e., clusters of four sites $\boldsymbol{w}_n = (w_n^{(1)}, w_n^{(2)}, w_n^{(3)}, w_n^{(4)})^T$, whose examples are shown in fig. 5. To describe the network in fig. 5(a), we can still adopt eq. (5), where

$$H = \begin{pmatrix} \mu - i\gamma & 1 & 0 & 0 \\ 1 & \mu - i\gamma & 1 & 0 \\ 0 & 1 & \mu + i\gamma & 1 \\ 0 & 0 & 1 & \mu + i\gamma \end{pmatrix}, \qquad (13)$$

the nonlinearity is given by

$$F(\boldsymbol{w}_n) = \mathrm{diag}\left(|w_n^{(1)}|^2, |w_n^{(2)}|^2, |w_n^{(3)}|^2, |w_n^{(4)}|^2\right),$$

and $\sigma_\pm$ are now 4×4 matrices whose only nonzero elements are $(\sigma_-)_{14} = (\sigma_+)_{41} = \epsilon$. The matrix H is invertible unless $\mu^2 = \frac{3}{2} - \gamma^2 \pm \frac{1}{2}\sqrt{5 - 16\gamma^2}$.

In the anticontinuum limit, defined by $\epsilon = 0$, the network shown in fig. 5(a) consists of a set of disconnected $\mathcal{PT}$-symmetric quadrimers. Here we consider the simplest case, when at $\epsilon = 0$ only one central quadrimer is excited, i.e., $\boldsymbol{w}_n = 0$ for $n \neq 0$, and look for continuation of this solution to $\epsilon > 0$.

To prove the possibility of analytical continuation as above, we concentrate on $\mathcal{PT}$-symmetric solutions (i.e., obeying the symmetry $w_n^{(1)} = \bar{w}_{-n}^{(4)}$ and $w_n^{(2)} = \bar{w}_{-n}^{(3)}$). This allows us to restrict the consideration to the semi-infinite matrices with $n \geqslant 0$. Moreover the invertibility of H for $\mu^2 \neq \frac{3}{2} - \gamma^2 \pm \frac{1}{2}\sqrt{5 - 16\gamma^2}$ ensures the continuation provided the Jacobian matrix for the central quadrimer is invertible.
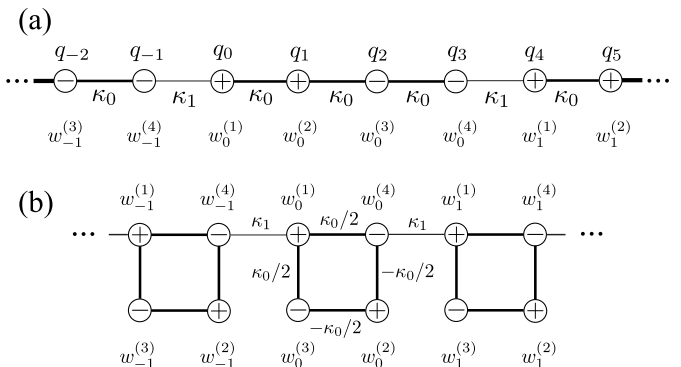

Fig. 5: Two examples of $\mathcal{PT}$-symmetric networks, which consist of a set of disconnected quadrimers in the anticontinuum limit.

For $n = 0$ and $\epsilon = 0$, the central quadrimer obeys the system of four equations (see eq. (5)),

$$H\boldsymbol{w}_0 = F(\boldsymbol{w}_0)\boldsymbol{w}_0, \qquad (14)$$

under the symmetry $w_0^{(1)} = \bar{w}_0^{(4)}$ and $w_0^{(2)} = \bar{w}_0^{(3)}$. While the nonlinear system (14) generally does not admit an explicit analytical solution (in contrast to the dimer case (7)), its properties are well studied. In particular, families of its nonlinear modes, bifurcation diagrams, and some exact solutions have been reported [12–14].

The network in fig. 5(a) is characterized by two types of the $\mathcal{PT}$ symmetry, the *local* and *global* ones. We say that the lattice is locally $\mathcal{PT}$-symmetric if the system (14) is $\mathcal{PT}$-symmetric in the limit $\epsilon = 0$. On the other hand, we say that the lattice is globally $\mathcal{PT}$-symmetric if the infinite network (5) with the matrix H in (13) is $\mathcal{PT}$-symmetric for $\epsilon \neq 0$. The network in fig. 5(a) consists of quadrimers which have unbroken local $\mathcal{PT}$ symmetry, at least for small γ. For $\epsilon > 0$ the infinite system has unbroken global $\mathcal{PT}$ symmetry allowing for stable discrete solitons. An example of a stable discrete soliton for this network is shown in fig. 6(a).

We shall now consider the network, which consists of clusters whose local $\mathcal{PT}$ symmetry is broken. However, proper choice of the coupling $\epsilon > 0$ makes the infinite network possess unbroken global $\mathcal{PT}$ symmetry. An example of such network is presented in fig. 5(b). For this network, we can still work with eq. (5), where

$$H = \begin{pmatrix} \mu - i\gamma & 0 & 1/2 & 1/2 \\ 0 & \mu - i\gamma & -1/2 & -1/2 \\ 1/2 & -1/2 & \mu + i\gamma & 0 \\ 1/2 & -1/2 & 0 & \mu + i\gamma \end{pmatrix}. \qquad (15)$$

Local $\mathcal{PT}$ symmetry is broken for any γ because eigenvalues of H are complex for any $\gamma > 0$. (We notice that the local $\mathcal{PT}$ symmetry can be fixed if we add the diagonal matrix $\mathrm{diag}(1, -1, 1, -1)$ to H. In this case, both networks shown in fig. 5 have equal spectra [13]).

The operator H is invertible unless $\mu = \pm\sqrt{1/2 - \gamma^2}$ or $\mu = \gamma = 0$. The existence of analytical continuation of the one-quadrimer state from $\epsilon = 0$ can be shown using the same ideas as the presented above. The only essential
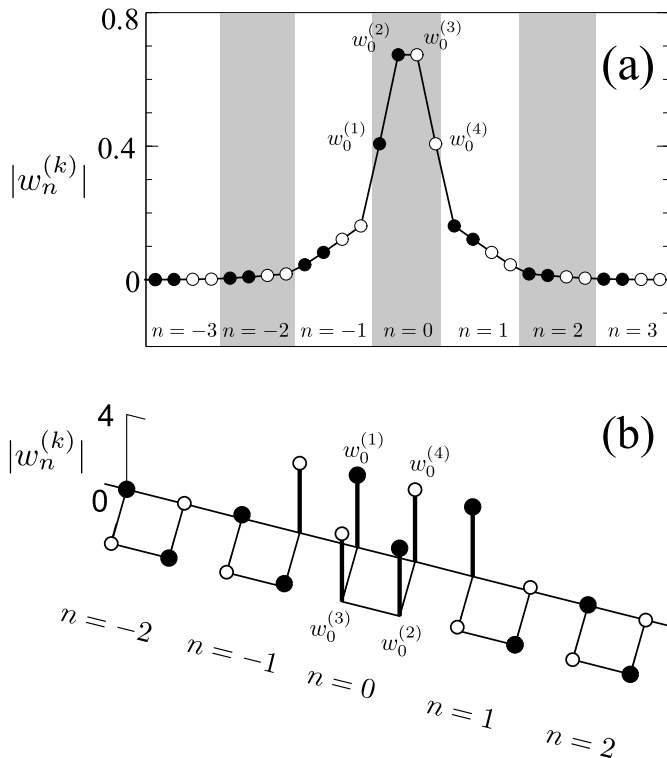
Fig. 6: (a) Stable soliton for the network in fig. 5(a) at $\epsilon = 0.5$, $\gamma = 0.25$ and $\mu = 2$. (b) Stable soliton for the network in fig. 5(b) at $\epsilon = 1.6$, $\gamma = 0.1$ and $\mu = 10$. Filled (empty) circles correspond to sites with gain (losses).

difference is that $\mathcal{PT}$-symmetric reduction is now given as follows: at the central quadrimer, we set $w_0^{(1)} = -\bar{w}_0^{(4)}$ and $w_0^{(2)} = \bar{w}_0^{(3)}$, while for $n \neq 0$, we set $w_n^{(1)} = -\bar{w}_{-n}^{(4)}$ and $w_n^{(2)} = \bar{w}_{-n}^{(3)}$.

Because local $\mathcal{PT}$ symmetry is broken for any γ, the global $\mathcal{PT}$ symmetry of the infinite network is also broken for small ϵ. Therefore, all the solitons bifurcating from the anticontinuum limit are unstable at least for sufficiently small ϵ. However, by increasing the coupling parameter ϵ, the global $\mathcal{PT}$ symmetry is restored and the network in fig. 5(b) may possess stable solitons. An example of a stable discrete soliton for this network is shown in fig. 6(b).

Conclusion. – In this letter we have shown that the idea of analytical continuation from the anticontinuum limit can be extended to the networks of $\mathcal{PT}$-symmetric clusters, offering the analytical proof of the existence of localized discrete solitons. Such solitons obey the $\mathcal{PT}$-symmetric shape and can be found stable. As particular examples, we considered in detail the chains of $\mathcal{PT}$-symmetric dimers and the networks of $\mathcal{PT}$-symmetric quadrimers.

The considered systems allow for further straightforward generalizations, say to chains of clusters where there exists more than one link among the neighbor ones, like the chain of dimers with pairwise coupling considered in [23] or the chain of oligomers, *i.e.*, clusters with more than four

sites. Furthermore, the approach of continuation from the anticontinuum limit can be used for developing a classification of intrinsic localized modes, as well as an analytical theory of the nonlinear stability of such modes.

$$* * *$$

REFERENCES

[1] Sievers A. J. and Takeno S., *Phys. Rev. Lett.*, **61** (1988) 970; Page J. B., *Phys. Rev. B*, **41** (1990) 7835.
[2] MacKay R. S. and Aubry S., *Nonlinearity*, **7** (1994) 1623.
[3] Lederer F. *et al.*, *Phys. Rep.*, **463** (2008) 1.
[4] Kevrekidis P. G. and Frantzeskakis D. J., *Mod. Phys. Lett. B*, **18** (2004) 173; Brazhnyi V. A. and Konotop V. V., *Mod. Phys. Lett. B*, **18** (2004) 627.
[5] Hennig D. and Tsironis G., *Phys. Rep.*, **307** (1999) 333; Kevrekidis P. G., *The Discrete Nonlinear Schrödinger Equation* (Springer, Berlin, Heidelberg) 2009.
[6] Eilbeck J. C., Lomdahl P. S. and Scott A. C., *Phys. Rev. B*, **30** (1984) 4703.
[7] Chen Y., Snyder A. W. and Pain D. N., *IEEE J. Quantum Electron.*, **28** (1992) 239.
[8] Ruschhaupt A., Delgado F. and Muga J. G., *J. Phys. A: Math. Gen.*, **38** (2005) L171.
[9] Bender C. M. and Boettcher S., *Phys. Rev. Lett.*, **80** (1998) 5243.
[10] Rüter C. E. *et al.*, *Nat. Phys.*, **6** (2010) 192.
[11] Ramezani H. *et al.*, *Phys. Rev. A*, **82** (2010) 043803; Sukhorukov A. A., Xu Z. and Kivshar Yu. S., *Phys. Rev. A*, **82** (2010) 043818.
[12] Li K. and Kevrekidis P. G., *Phys. Rev. E*, **83** (2011) 066608.
[13] Zezyulin D. A. and Konotop V. V., *Phys. Rev. Lett.*, **108** (2012) 213906.
[14] Li K., Kevrekidis P. G., Malomed B. A. and Günther U., *J. Phys. A: Math. Theor.*, **45** (2012) 444021.
[15] Bendix P., Fleischmann R., Kottos T. and Shapiro B., *Phys. Rev. Lett.*, **103** (2009) 030402.
[16] Dmitriev S. V., Sukhorukov A. A. and Kivshar Yu. S., *Opt. Lett.*, **35** (2010) 2976.
[17] Musslimani Z. H. *et al.*, *Phys. Rev. Lett.*, **100** (2008) 030402; Nixon S., Ge L. and Yang J., *Phys. Rev. A*, **85** (2012) 030402.
[18] He Y. *et al.*, *Phys. Rev. A*, **85** (2012) 013831.
[19] Abdullaev F. Kh. *et al.*, *Phys. Rev. A*, **83** (2011) 041805.
[20] Alfimov G. L., Brazhnyi V. A. and Konotop V. V., *Physica D*, **194** (2004) 127.
[21] Barashenkov I. V., Bogdan M. M. and Korobov V. I., *Europhys. Lett.*, **15** (1991) 113.
[22] Barashenkov I. V., Zemlyanaya E. V. and Bär M., *Phys. Rev. E*, **64** (2001) 016603.
[23] Suchkov S. V., Malomed B. A., Dmitriev S. V. and Kivshar Yu. S., *Phys. Rev. E*, **84** (2011) 046609.